IUGG IASPEI International Association of Seismology and Physics of the Earth's Interior

IUGG IAGA International Association of Geomagnetism and Aeronomy

31 August - 5 September 2025
Lisbon, Portugal

Fabry Pérot observations of the thermospheric winds using various retrieval methods over Tenerife

Arthur Gauthier[1,2,3], Christopher Geach[3], Gunter Stober[1,2], Claudia Borries[3]

1 Institute of Applied Physics, University of Bern, 2 Oeschger Center for Climate Change Research, University of Bern, 3 Institute for Solar-Terrestrial Physics, German Aerospace Center (DLR), Neustrelitz, Germany

DLR-SOFPIT Instrument

- The Fabry-Pérot Interferometer (FPI) SOFPIT observes the 630.0 nm line airglow emission from altitudes around 200–300 km.
- The FPI creates interference ring patterns that vary with the observed wavelength due to the Doppler shift. The FPI retrieves the line-of-sight wind velocity and temperature of the emitting particles.

Component	Specification
Sky Scanner	From KEO Scientific: views in 4 cardinal directions + zenith + laser
Filter	630 nm (red oxygen emission line)
Etalon	Diameter: 116 mm Thickness: 15 mm Reflectivity: R = 0.76
Calibration	HeNe laser
Imaging Optics	Focal length: 300 mm
CCD Detector	Size: 13.312 mm × 13.312 mm Resolution: 1024 × 1024 pixels

Tab1. Key elements of SOFPIT

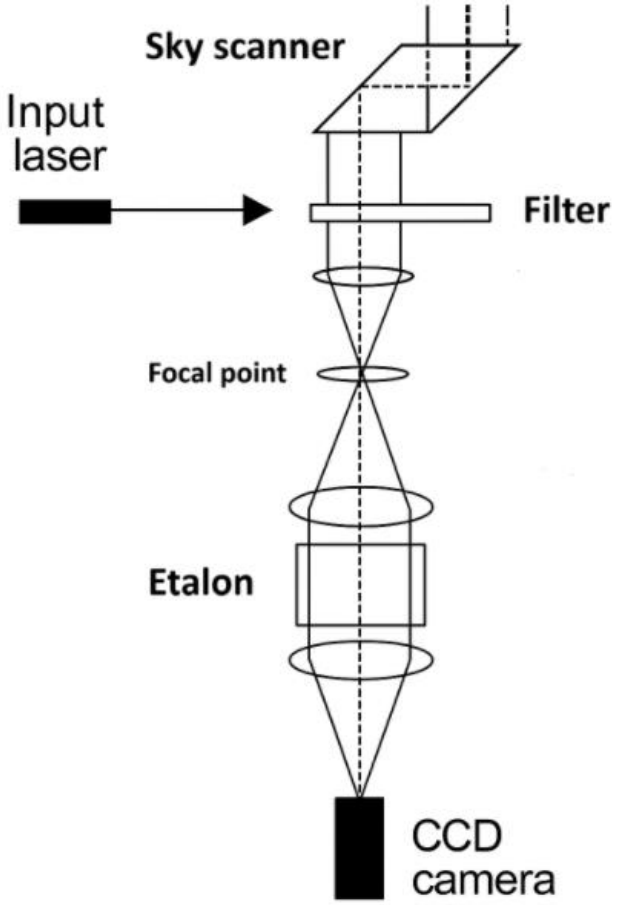

Fig1. Schematic diagram of SOFPIT

SOFPIT Measurement process

- A full sky scan (east, west, north, south, vertical, laser) is performed with 3 minutes exposures and 15-second readout intervals per direction.

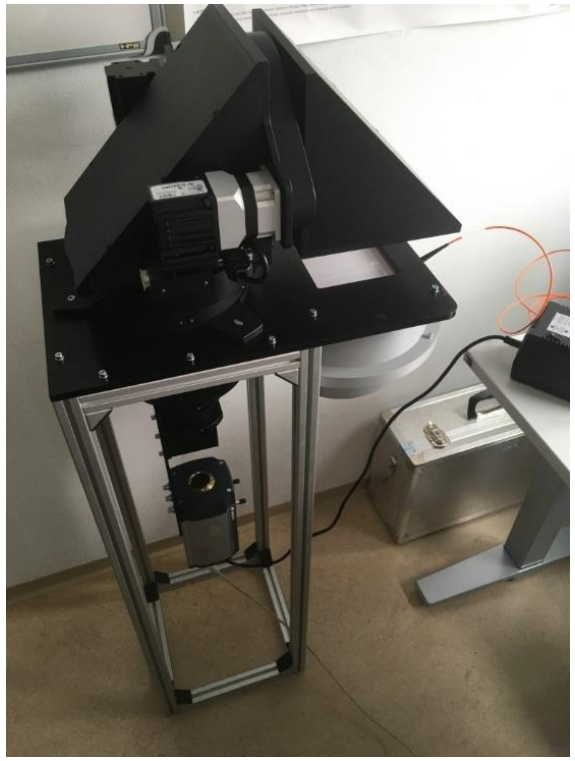

Fig2. SOFPIT

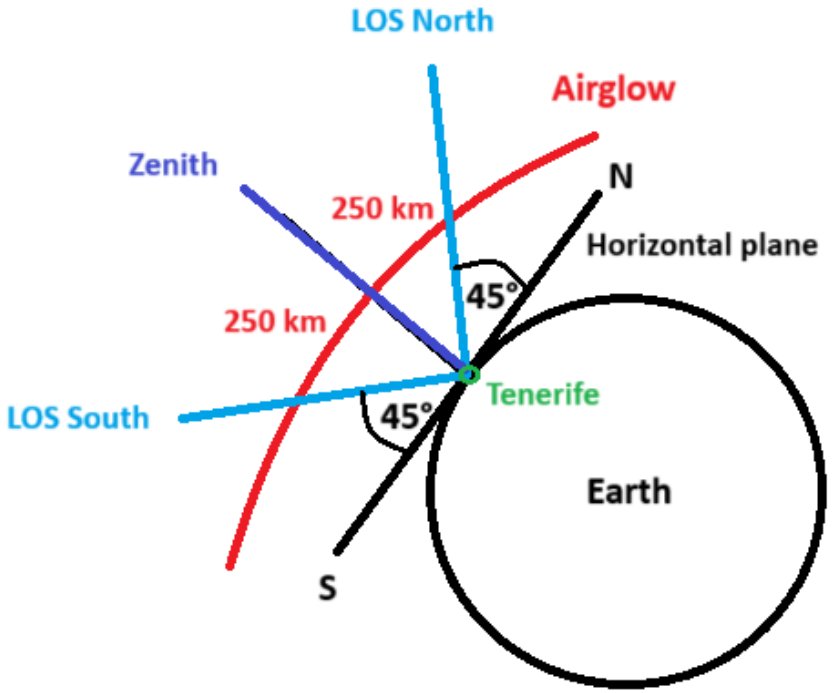

Fig3. Measurement setup diagram

Fig4. Container with SOFPIT on Tenerife

Method for Horizontal Wind Retrieval: Shiokawa Method

- **Assumptions**: Horizontal wind is uniform between two opposite viewing directions (~500 km apart)
- **Method**: Wind velocity is determined by comparing fringe patterns from Fabry–Perot Interferometer images taken in opposite directions (north–south or east–west), based on the shift in fringe center positions.
- **Result**: Each image provides multiple wind estimates, which are averaged to yield a single meridional or zonal wind value, following the method of Shiokawa et al. (2012).

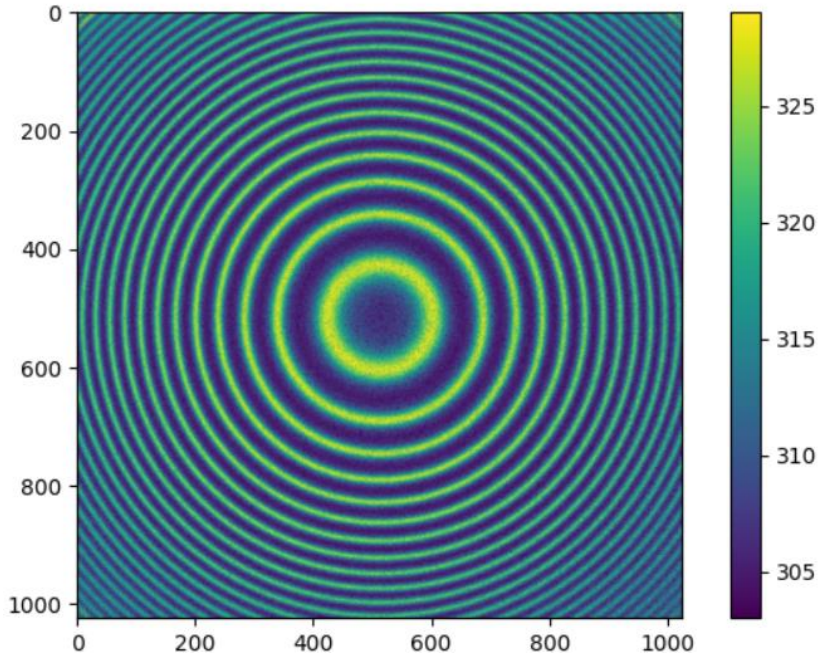

Fig5. Real Sky image

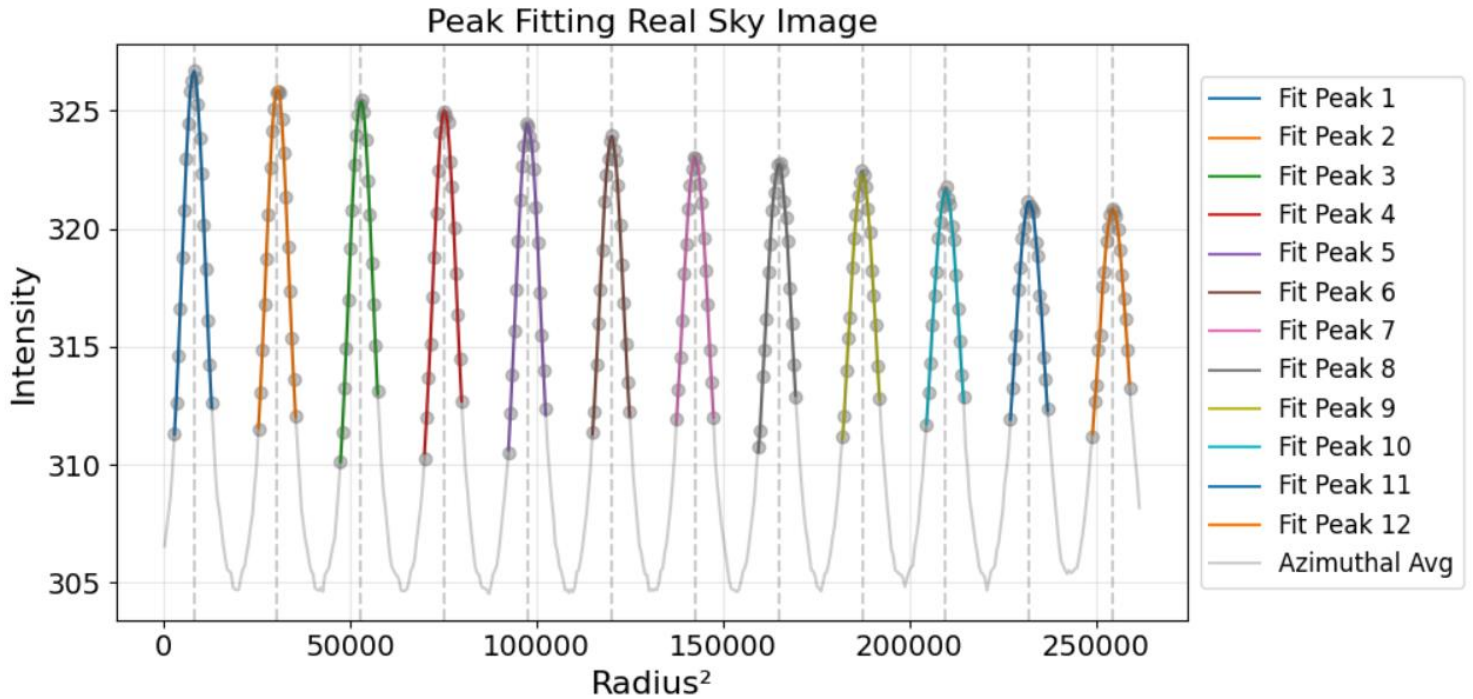

Fig6. Peak Detection via Azimuthal Averaging and Fitting

Result of the Shiokawa Method : Horizontal winds for night of 26/10/2024

Wind calculation:

$$v_N = \frac{c}{\cos\Theta}\frac{(r_S^2 - r_N^2)}{\left(4f^2 - (r_N^2 + r_S^2)\right)}$$

Shiokawa et al. (2012)

Wind Error Estimation:

$$Error = \frac{std(N)}{\sqrt{N-1}}$$

where N = number of detected peaks.

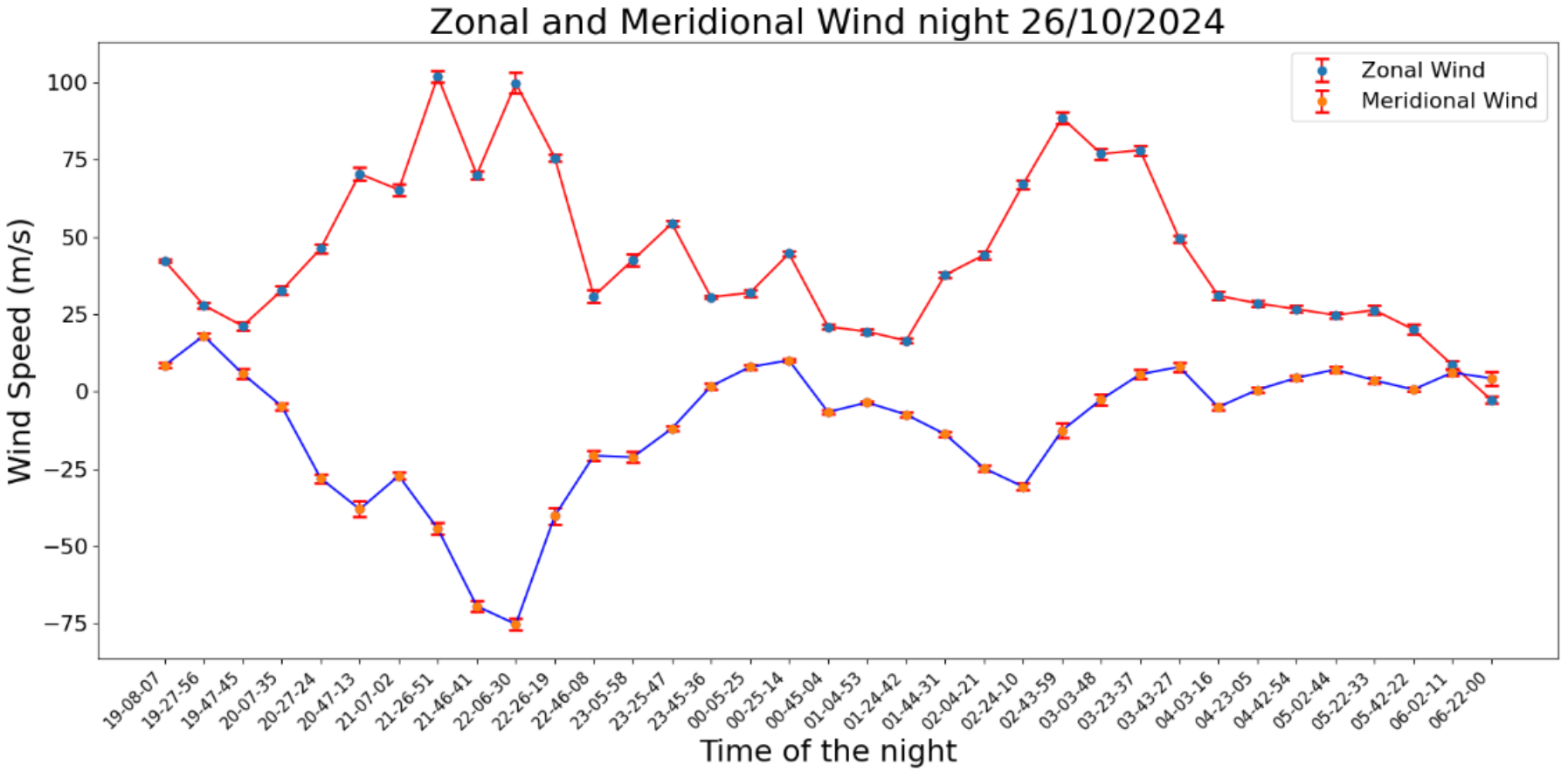

Fig7. Zonal and meridional winds night of 26/10/2024

Forward Model and Inversion Method: Harding method

Forward laser (632.8nm) model calibration fringes:

- **Assumption:** average vertical wind is zero across a night of measurements, and vertical wind components are negligible in each individual measurement.
- Following the method of Harding et al. (2014): Model for Laser Calibration Fringes:

$$A(r,\lambda) = \frac{I}{1 + \frac{4R}{(1-R)^2}\sin\left(\frac{2\pi nd}{\lambda}\cos(\arctan(\frac{r}{f}))\right)^2}$$

- Modulation in intensity for attenuations of the fringes at the edges of the CCD: $I = I_0(1 + I_1\frac{r}{r_{max}})$
- Implementation of a point spread function where each pixel becomes a weighted average of the neighborhood pixels of the ideal Airy function: This simulates the effects of the optical defects:

$$b(s,r) = \frac{1}{\sqrt{2\pi\sigma(r)^2}} e^{\frac{(s-r)^2}{\sigma(r)^2}} \text{ with } \sigma(r) = \sigma_0 + \sigma_1 \sin\left(\pi\frac{r}{r_{max}}\right) + \sigma_2\cos(\pi\frac{r}{r_{max}})$$

- The method consists in determining the best value for the free parameters to fit the laser calibration fringes.

Forward model for laser calibration fringes

Parameters	Description
Average intensity I_0	Average intensity of the laser fringes
Linear falloff of intensity I_1	Rate at which intensity decreases linearly
Average blur size σ_0	Mean size of the blur function
Sin-variation of blur size σ_1	Sinusoidal variation of the blur size
Sin-variation of blur size σ_2	Cosine variation of the blur size
Etalon gap d	Physical gap between the etalon plates
Focal length f	Focal length of the optical system
Background B	Background intensity level in the image

Tab2. Instrumental variables for estimation

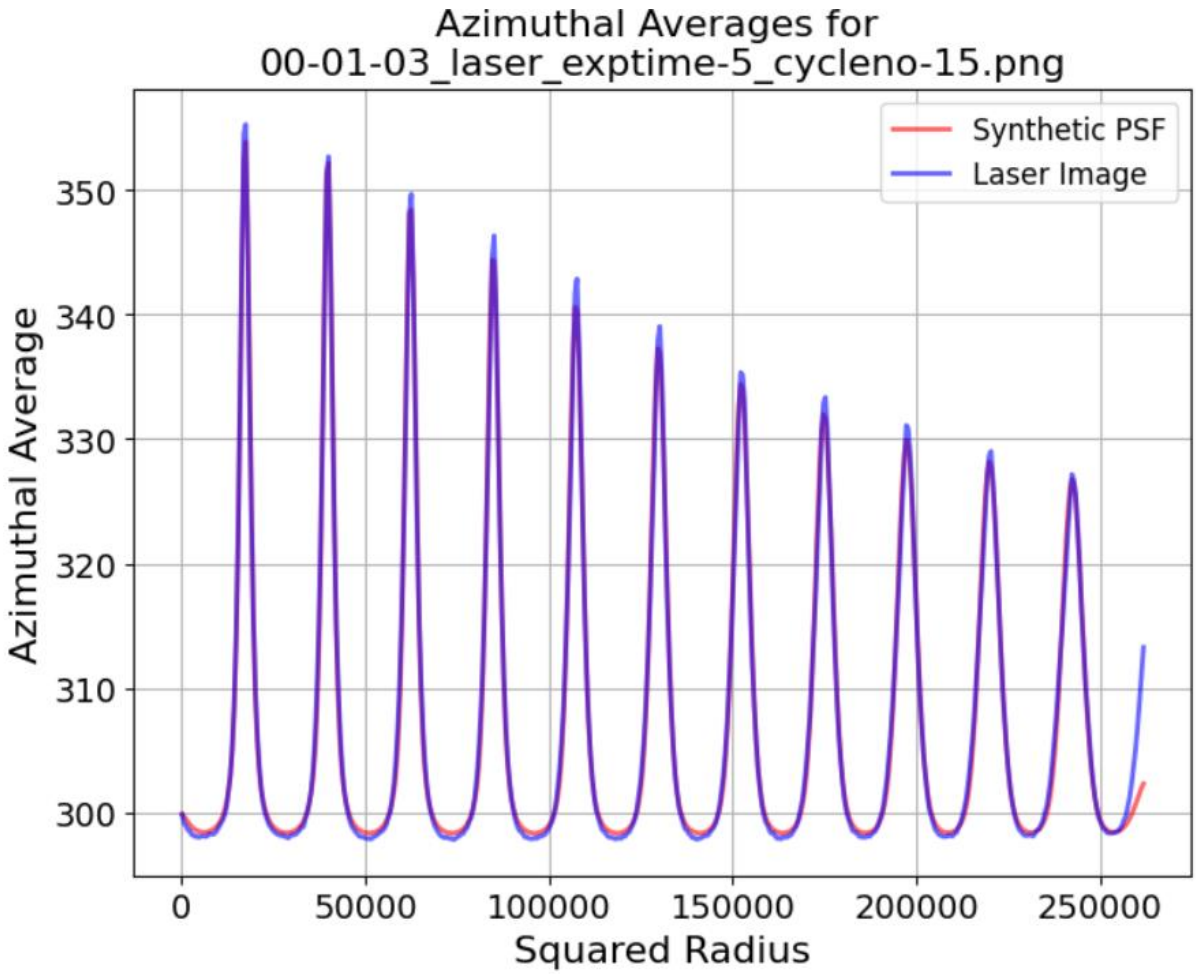

Fig7. Assessment of fit quality of the Laser model

Forward model for airglow fringes

- The forward model for airglow fringes uses the same equations, but replaces the delta function from the laser with a source spectrum that is a thermally broadened and Doppler shifted Gaussian:

$$Y(\lambda) = Y_{bg} + Y_{line} exp\left\{-\frac{1}{2}\left(\frac{\lambda - \lambda_c}{\Delta\lambda}\right)^2\right\}$$

- The airglow model inputs include $\lambda_c, \Delta\lambda, Y_{bg}, Y_{line}, and\ B$. These physical parameters are the target of optimization.

- Velocities and Temperatures :

$$\lambda_c = \lambda_0\left(1 + \frac{v}{c}\right) \text{ and } \Delta\lambda = \frac{\lambda_0}{c}\sqrt{\frac{kT}{m}}$$

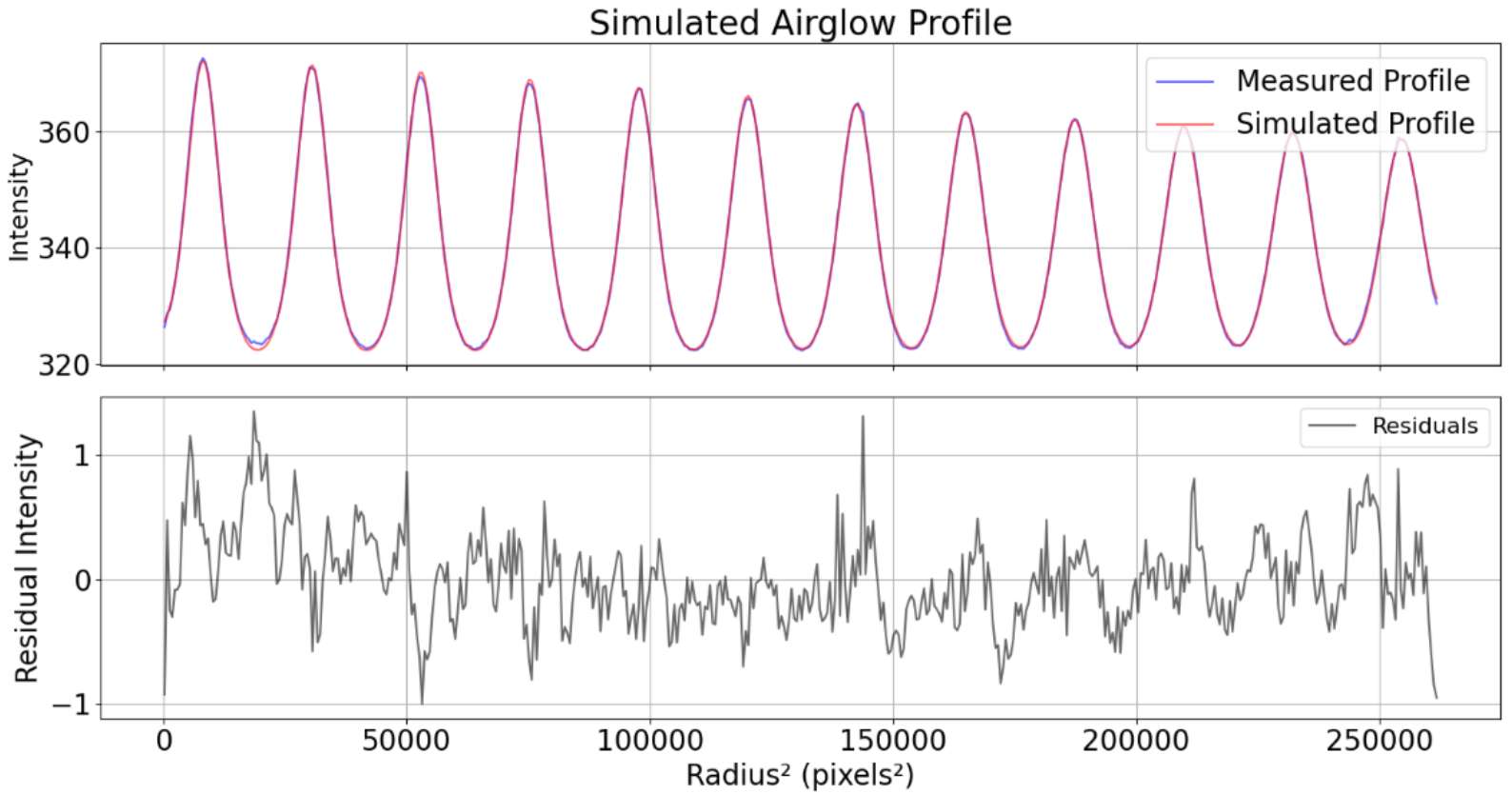

Fig8. Assessment of fit quality of the Airglow model

First comparison of Horizontal Wind Retrievals

Zonal Winds on the Night of 26–27 October 2024

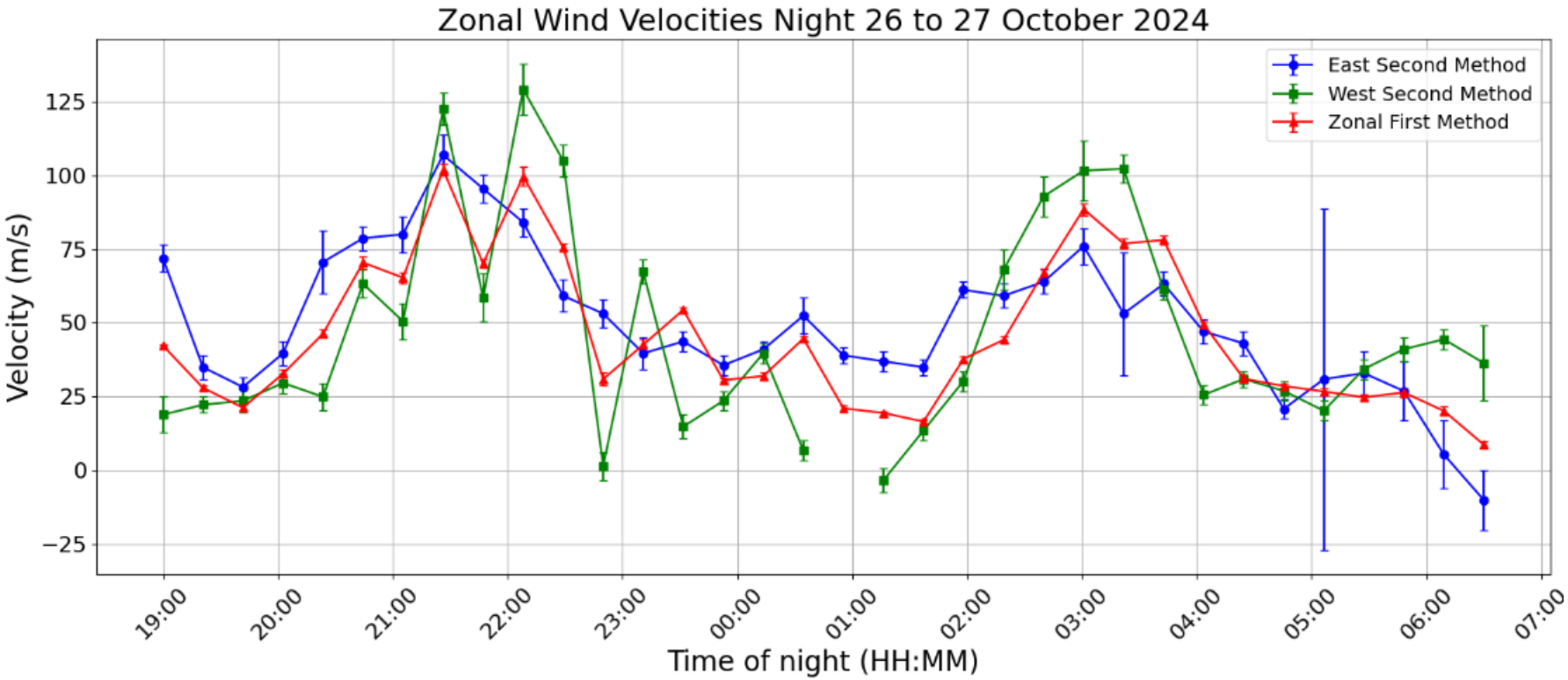

Fig9. Comparison zonal winds for the 2 retrieval methods

- The Shiokawa method assumes uniform winds over ~500km. Harding method permits to analyze each beam separately.
- The difference between the profiles indicates large-scale gradients in the wind field and increased measurement uncertainties.

First comparison of Horizontal Wind Retrievals

Meridional Winds on the Night of 26–27 October 2024

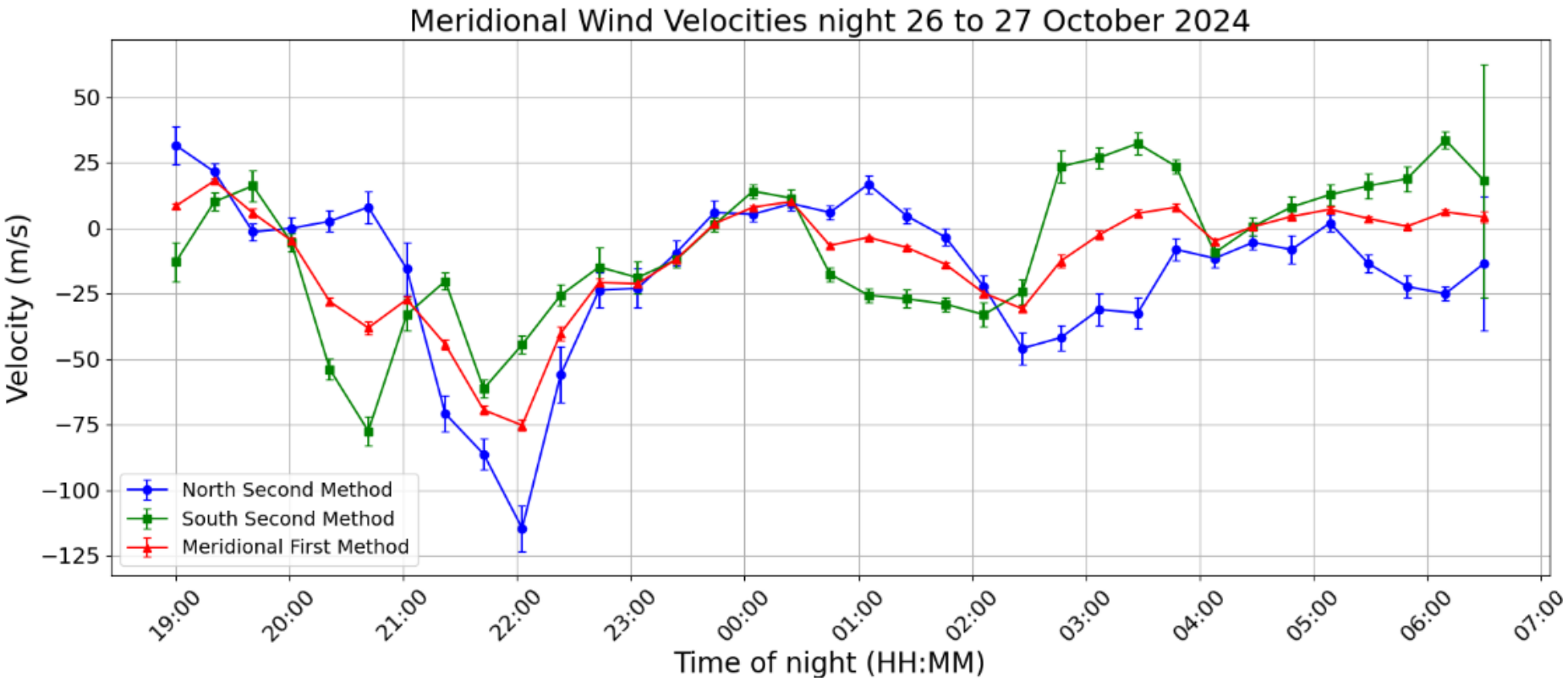

Fig10. Comparison meridional winds for the 2 retrieval methods

- Differences in local wind conditions can cause the retrieval methods to diverge.
- The Shiokawa method wind retrieval then reflects a spatial average of the Harding wind retrieval method.

Discussion and further steps

- Define criteria for valid measurements, e.g., applying a cutoff based on the standard deviation of residuals.
- Retrieve the winds in both methods for longer periods, not just individual days.
- Assess the sensitivity of retrieved velocities to small perturbations in instrumental parameters and for a larger dataset (for example, etalon gap).
- Test the zero-wind hypothesis: can vertical winds be assumed negligible over one night, and horizontal winds considered uniform between two opposite viewing directions (~500 km apart)?

Conclusions

- Obtention of winds measurements in the thermosphere above the Canary Islands.
- Retrieval of winds through 2 different retrieval methods.
- The Shiokawa method wind retrieval reflects a spatial average of the winds retrieved in opposite directions in the Harding wind retrieval method.

Conclusions

- Obtention of winds measurements in the thermosphere above the Canary Islands.
- Retrieval of winds through 2 different retrieval methods.
- The Shiokawa method wind retrieval reflects a spatial average of the winds retrieved in opposite directions in the Harding wind retrieval method.

Thank you for your attention

Email: arthur.gauthier@dlr.de